The Plant Cell, Vol. 32: 2951–2963, September 2020, www.plantcell.org © The authors.

Synergy among Exocyst and SNARE Interactions Identifies a Functional Hierarchy in Secretion during Vegetative Growth[CC-BY]

Emily R. Larson,[a,1,2] Jitka Ortmannová,[b,1,3] Naomi A. Donald,[a] Jonas Alvim,[a] Michael R. Blatt,[a,4] and Viktor Žárský[b,c]

[a] Laboratory of Plant Physiology and Biophysics, Bower Building, University of Glasgow, Glasgow G12 8QQ, United Kingdom
[b] Institute of Experimental Botany, Academy of Sciences of the Czech Republic, 165 02 Prague 6, Czech Republic
[c] Department of Experimental Plant Biology, Faculty of Science, Charles University, 128 44 Prague 2, Czech Republic

Vesicle exocytosis underpins signaling and development in plants and is vital for cell expansion. Vesicle tethering and fusion are thought to occur sequentially, with tethering mediated by the exocyst and fusion driven by assembly of soluble NSF attachment protein receptor (SNARE) proteins from the vesicle membrane (R-SNAREs or vesicle-associated membrane proteins [VAMPs]) and the target membrane (Q-SNAREs). Interactions between exocyst and SNARE protein complexes are known, but their functional consequences remain largely unexplored. We now identify a hierarchy of interactions leading to secretion in Arabidopsis (*Arabidopsis thaliana*). Mating-based split-ubiquitin screens and in vivo Förster resonance energy transfer analyses showed that exocyst EXO70 subunits bind preferentially to cognate plasma membrane SNAREs, notably SYP121 and VAMP721. The *exo70A1* mutant affected SNARE distribution and suppressed vesicle traffic similarly to the dominant-negative truncated protein SYP121$^{\Delta C}$, which blocks secretion at the plasma membrane. These phenotypes are consistent with the epistasis of *exo70A1* in the *exo70A1 syp121* double mutant, which shows decreased growth similar to *exo70A1* single mutants. However, the *exo70A1 vamp721* mutant showed a strong, synergy, suppressing growth and cell expansion beyond the phenotypic sum of the two single mutants. These data are best explained by a hierarchy of SNARE recruitment to the exocyst at the plasma membrane, dominated by the R-SNARE and plausibly with the VAMP721 longin domain as a nexus for binding.

INTRODUCTION

Exocytosis depends on the spatiotemporal formation, delivery, and fusion of membrane vesicles that distribute their cargos to the plasma membrane and apoplast. Proteins that regulate exocytotic mechanics include the exocyst complex, which tethers and docks vesicles to target membranes (TerBush et al., 1996; Zarský et al., 2009; Vukašinović and Žárský, 2016), and soluble NSF attachment protein receptor (SNARE) protein complexes that drive the final steps of vesicle fusion (Jahn and Scheller, 2006; Bassham and Blatt, 2008; Südhof and Rothman, 2009). Structural protein models suggest the exocyst assembles as a set of helical bundles (Picco et al., 2017; Mei et al., 2018) that are evolutionary conserved and comprise eight subunits (TerBush et al., 1996; Zarský et al., 2013): SEC3, SEC5, SEC6, SEC8, SEC10, SEC15, EXO70, and EXO84. The EXO70 family of subunits in land plants shows substantial gene expansion, with 23 paralogues in Arabidopsis (*Arabidopsis thaliana*) that may reflect specialization in the maintenance of different tethering domains (Synek et al., 2006; Cvrčková et al., 2012).

SNARE proteins are classified by the Q or R amino acid residue found at the core of the interacting assembly and localize to vesicle (R-SNAREs or vesicle-associated membrane proteins [VAMPs]) and target (Qa-, Qb-, and Qc-SNAREs) membranes (Fasshauer et al., 1998; Blatt and Thiel, 2003; Jahn and Scheller, 2006). SNARE function is conserved within eukaryotes, but these gene families are similarly expanded in land plants consistent with evolutionary specialization (Sanderfoot et al., 2000; Blatt and Thiel, 2003; Pratelli et al., 2004). The Qa-SNAREs, SYP121 and SYP122, have overlapping functions at the plasma membrane and are associated with accelerated traffic during growth as well as specialized functions in abiotic and biotic stress resistance (Grefen et al., 2015; Karnik et al., 2017; Waghmare et al., 2018). SYP121 and SYP122 assemble with cognate R-SNAREs VAMP721 and VAMP722 as functional complexes that fuse vesicles with the plasma membrane (Kwon et al., 2008, 2013; Karnik et al., 2015).

Current models differentiate temporally and mechanistically between vesicle tethering mediated by the exocyst and fusion mediated by the SNAREs to highlight the sequential functions of these protein complexes (Cai et al., 2007; Mei and Guo, 2019). Nonetheless, with the spatial and functional proximities of the two complexes, increasing evidence for interactions between subunits of the separate complexes has surfaced. Several exocyst subunits in yeast interact with SNAREs in vitro or affect their localization within the cell (Sivaram et al., 2005; Morgera et al., 2012; Shen et al., 2013; Yue et al., 2017), leading to the idea of a coordination between exocyst and SNARE complexes at the plasma membrane (Picco et al., 2017; Mei and Guo, 2019). In Arabidopsis,

[1] These authors contributed equally to this work.
[2] Current address: Root Development Research Group, School of Biological Sciences, University of Bristol, Bristol Life Sciences Building, 24 Tyndall Avenue, Bristol BS8 1TQ, United Kingdom.
[3] Current address: Uppsala Biocenter, SLU, Department of Plant Biology, PO Box 7080, SE-19 750 07 Uppsala, Sweden.
[4] Address correspondence to michael.blatt@glasgow.ac.uk.
The author responsible for distribution of materials presented in this article in accordance with the policy described in the Instructions for Authors (www.plantcell.org) is: Michael R. Blatt (michael.blatt@glasgow.ac.uk).

www.plantcell.org/cgi/doi/10.1105/tpc.20.00280

IN A NUTSHELL

Background: Cells use vesicles to transport cargo throughout the cell and to the plasma membrane, which is critical for plant cell growth and function. Several different proteins help control and regulate vesicle traffic to deliver cellular cargo to its functional locations. During secretion, SNARE proteins located on the vesicle and plasma membrane interact to fuse the two membranes together and deposit the protein cargo. While SNAREs are required for membrane fusion, they rely on other mechanisms to get the vesicles in proximity to their target membranes. The exocyst is a well-studied tethering complex that helps deliver vesicles to the plasma membrane. Although it has been hypothesized that SNARE and exocyst protein complexes work in the same secretory pathways, there is a lack of *in vivo* evidence of interactions between either protein subunits or complexes in plants.

Question: We hypothesized that there are direct interactions between SNARE and exocyst proteins that support cargo delivery at the plasma membrane, and that these interactions could happen in a sequential manner to regulate vesicle delivery and fusion.

Findings: Using split-ubiquitin yeast mating and FRET analyses, we identified direct interactions between the EXO70A1 exocyst subunit and SNAREs on both the vesicle (VAMP721) and plasma membrane (SYP121). We found that the *exo70a1* mutant has reduced secretion, consistent with the redistribution of the vesicle SNARE VAMP721 away from the plasma membrane in the *exo70a1* mutant background. These results suggest that the exocyst helps deliver or recruit vesicles to the plasma membrane through its interactions with SNARE proteins. In the *syp121 exo70a1* double mutant, *syp121* was epistatic to *exo70a1* but surprisingly, the *vamp721 exo70a1* double mutant had synergistic phenotypes, including severe growth suppression. We believe that these results indicate a functional hierarchy between vesicle and plasma membrane SNAREs and highlight the consequences of these interactions on plant growth.

Next steps: We know the protein domain of VAMP721 that is important for its interactions with EXO70A1, we would now like to know what part of EXO70A1 regulates its interactions with SNARE proteins and how they support the dynamics of vesicle delivery at the plasma membrane.

the exocyst EXO70B1 and EXO70B2 subunits interact in vitro with the SNAP33 subunit of the plasma membrane SNARE complex (Pecenková et al., 2011), although the significance of these interactions in vivo is unknown.

One difficulty is the paucity of in vivo data that might speak to the physiological consequences of exocyst and SNARE subunit interactions, especially in plants. Inhibiting SNARE function has been shown to disrupt exocytosis in Arabidopsis and other plant models (Geelen et al., 2002; Tyrrell et al., 2007; Karnik et al., 2013; Grefen et al., 2015), and impairing exocyst function affects growth and, in some instances, SNARE distributions within cells (Fendrych et al., 2013; Synek et al., 2017). These observations are consistent with the concept of serial processing from tethering through to vesicle fusion. What has been missing is evidence arising from an interaction between one or more exocyst and SNARE subunits that surpasses any functional consequences of the subunits in isolation.

We report here the interactions of members of the EXO70 exocyst subfamily with SNARE proteins that drive vesicle fusion at the plasma membrane and the consequences for secretory vesicle traffic. We show that the omnipresent EXO70A1 exocyst subunit requires the so-called longin regulatory domain of the R-SNARE VAMP721 for interaction. Most important, we report that the loss of a subset of interactors among exocyst and SNARE proteins affecting vesicle traffic leads to synergistic impacts on cell expansion and vegetative growth that are unique to EXO70 interactions with the R-SNARE. The findings demonstrate a functional hierarchy in interactions between EXO70A1 with VAMP721 that suggest a handover of vesicles between exocyst and SNARE complexes that leads to vesicle fusion and establishes a landmark for further exploration of secretory mechanics in plants.

RESULTS

The Exocyst and SNARE Proteins Physically Interact

EXO70A1 associates dynamically with the plasma membrane, where it has been suggested to provide a landmark for vesicle docking. Indeed, VAMP721 localization is altered in the *exo70A1* mutant (Fendrych et al., 2013), consistent with this idea. To assess whether direct interactions between the exocyst and one or more SNAREs may underpin these processes, we used a yeast mating-based split-ubiquitin system (mbSUS; Grefen et al., 2015; Zhang et al., 2018). The mbSUS approach offers a number of advantages over yeast two-hybrid methods in allowing for analysis of interactions between full-length proteins, especially with integral membrane and membrane-associated proteins, and in screening weighted against false-positive interactions that facilitates comparisons of relative binding specificities (Zhang et al., 2015, 2018; Xing et al., 2016). We tested for interactions with four EXO70 subunits, including EXO70A1 that is widely expressed in the vegetative plant (Synek et al., 2006), EXO70H1, and two EXO70B subunits that have been associated with pathogen defense and autophagy (Pecenková et al., 2011; Kulich et al., 2013; Wang et al., 2020), challenging these with several plasma membrane–associated SNAREs (Figure 1; Supplemental Figure 1). Strong yeast growth was recovered, notably with EXO70A1 when paired with the plasma membrane Qa-SNAREs SYP121 and SYP122; the plasma membrane R-SNAREs VAMP721, VAMP722, VAMP724; and VAMP727, and to a lesser extent, with the cognate Qbc-SNARE SNAP33.

Increasing Met concentrations in the medium, to suppress bait expression and test the strength of interactions, showed that

EXO70A1 has a modest preference for SYP121 over SYP122 and for VAMP721 over VAMP722. It also showed no appreciable interaction with the endomembrane R-SNARE VAMP723, even though the R-SNARE was strongly expressed in each of the assays (Supplemental Figure 2), consistent with a specificity for components assembling in plasma membrane SNARE core complexes. Like EXO70A1, the cognate SNARES SYP121 and VAMP721 are widely expressed throughout the plant (Bassham and Blatt, 2008; Karnik et al., 2017; Waghmare et al., 2018). As these two SNAREs generally interacted most strongly with the EXO70 subunits, especially with the widely expressed EXO70A1 subunit of the exocyst, we focused on these interactors.

To assess the characteristics of exocyst binding with the R-SNARE, we compared interactions of EXO70A1 with VAMP721 and VAMP723. These R-SNAREs are 89% sequence identical and exhibit >94% similarity at the amino acid level (for R-SNARE protein alignment, see supplemental Figure 1 of Zhang et al. [2015]). Previous studies showed that domain exchanges between the longin domains of these R-SNAREs is sufficient to alter their binding with the plasma membrane K^+ channels KAT1 and KC1 and affect channel gating, effects that were traced to a single amino acid residue that differs between the two R-SNAREs (Zhang et al., 2015, 2017). Furthermore, a functional mapping of the putative binding surface exposed a secondary binding site for the K^+ channels that is common to both R-SNAREs (Zhang et al., 2017), thus arguing against substantial conformational differences between the two R-SNAREs and their mutations.

We used the same constructs of VAMP721 and VAMP723 incorporating the respective domain exchanges (Zhang et al., 2015, 2017) to explore the R-SNARE domains required for interaction with the EXO70A1 subunit bait. We observed yeast growth in mbSUS assays with VAMP723 only when the VAMP721 longin domain was substituted for that of VAMP723; conversely, yeast growth was lost when the longin domain of VAMP723 was substituted for the longin domain in VAMP721. A similar loss of interaction was also observed with the other EXO70 subunits, indicating that the VAMP721 longin domain incorporates an essential structural component determining EXO70 binding (Figure 1B; Supplemental Figures 3 and 4) much as it does for VAMP721 binding with the K^+ channels. The finding is of interest, because both R-SNARE partners have been proposed as plasma membrane landmarks affecting the final stages of vesicle fusion (Grefen et al., 2015; Karnik et al., 2017; Zhang et al., 2017).

To validate the EXO70 interactions in vivo, we used Förster resonance energy transfer (FRET) after transiently transforming *Nicotiana benthamiana* leaves with mCherry-EXO70A1 and several GFP-VAMP protein fusions under control of the 35S promoter. The constructs were incorporated within the pFRETgc-2in1 multicistronic vector to ensure equal genetic loads as well as provide markers for expression on a cell-by-cell basis (Hecker et al., 2015). These experiments were combined with mCherry-SYP121 and GFP-VAMP721 and with mCherry-EXO70A1 with free GFP (2xGFP) as positive and negative controls, respectively. To accommodate differences in fluorescence intensities of the protein fusions, we used the PixFRET method (Feige et al., 2005) that corrects for spectral bleed-through relative to fluorophore intensity and for bias arising from differences in fluorophore emission that would otherwise affect comparisons of FRET across

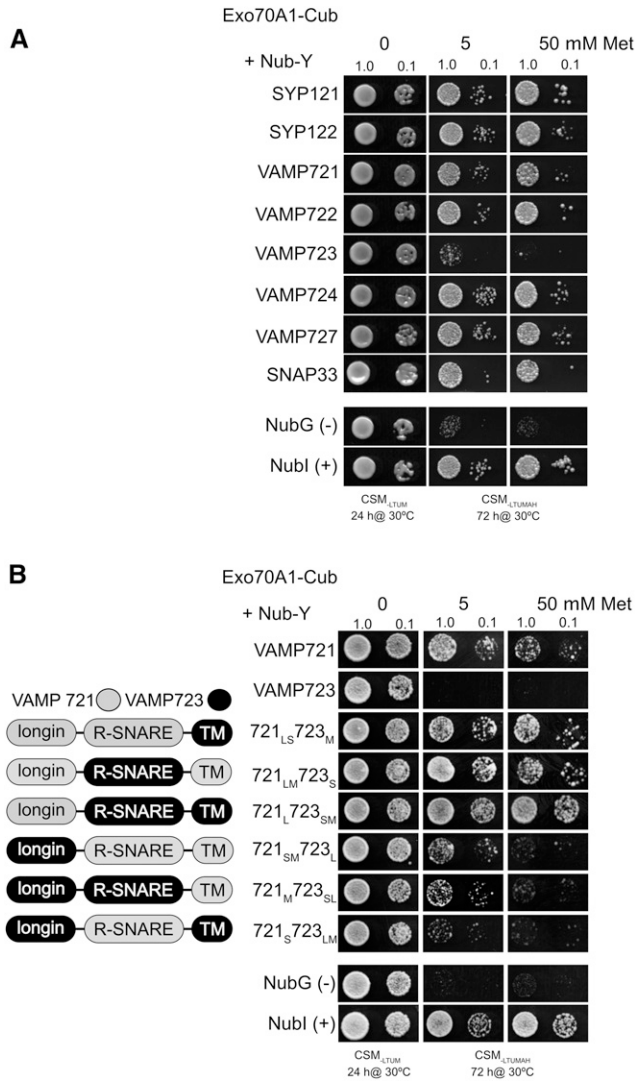

Figure 1. Exocyst EXO70 Subunits Interact Differentially with SNAREs Associated with Secretion at the Plasma Membrane.

(A) Yeast mbSUS assay for interaction of the OST4-anchored EXO70A1-Cub bait and Nub prey fusions with the SNARE proteins as indicated. Yeast dropped as 1.0× and 0.1× dilutions of 0.6 OD_{600} yeast suspensions and grown on selective synthetic medium lacking Leu, Trp, Ura, Met (CSM_{-LTUM}) as a control for mating and on the same medium additionally lacking Ala and His ($CSM_{-LTUMAH}$) as a test for bait and prey interaction. NubG and NubI were included as negative and positive prey controls, respectively. Growth on 5 and 50 μM Met to suppress bait expression tests for interaction specificity. Immunoblots confirming bait and prey expression are included in Supplemental Figure 3.

(B) mbSUS assay for EXO70A1 interactions as in **(A)** but with VAMP721/VAMP723 chimeras as indicated (left). Comparison of reciprocal domain exchanges indicate that the VAMP721 longin domain is required for interaction. Mated yeast dropped as 1.0× and 0.1× dilutions of 0.6 OD_{600} yeast suspensions. Immunoblots confirming bait and prey expression are included in Supplemental Figure 4. Both **(A)** and **(B)** are one of three independent experiments, all yielding similar results.

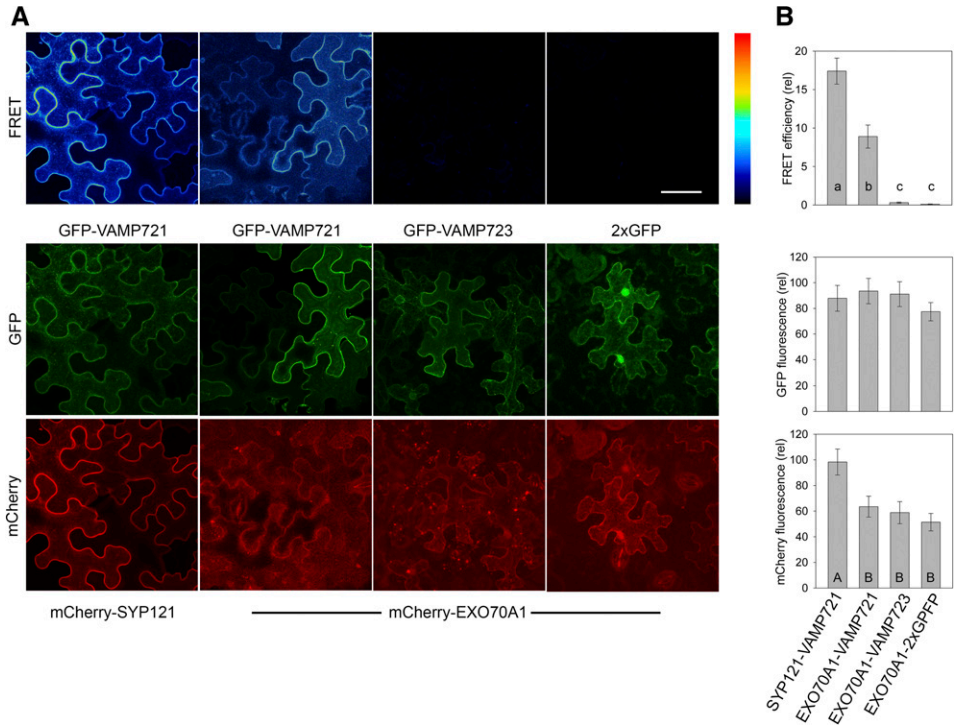

Figure 2. VAMP721 and EXO70A1 Interact in Vivo.

(A) FRET analysis on coexpressing mCherry-EXO70A1 and GFP-VAMP721, GFP-VAMP723 and 2xGFP in transiently transformed *N. benthamiana* leaf epidermis. Coexpression used the pFRETgc-2in1-NN multicistronic vector and quantification was with the PixFRET tool (Feige et al., 2005; Schindelin et al., 2012). The combinations of mCherry-SYP121 with GFP-VAMP721 and mCherry-SYP121 with 2xGFP were included as positive and negative controls, respectively. Images in the panel rows (top to bottom) are projections of image stacks analyzed for FRET, the GFP (donor) and mCherry (acceptor) fluorescence signals. The FRET analysis is pseudo-color–coded to the scale shown (right). A FRET signal was evident between EXO70A1 and VAMP721, but not VAMP723 or 2xGFP. Bar = 50 μm.

(B) Quantification of FRET efficiency (top) calculated from PixFRET grayscale outputs with correction for the relative intensities of GFP (donor) and mCherry (acceptor) fluorescence signals. Data are means ± SE of $n \geq 8$ independent experiments, with measurements in each experiment taken from the entire image planes of three to five randomly selected image sets. Quantification of GFP (donor) and mCherry (acceptor) fluorescence signals (middle and bottom, respectively) are for the same data sets and show no significant difference in donor fluorescence. No significant differences between mCherry-EXO70A1 fluorescence signals were observed, and only the mCherry-SYP121 fluorescence was stronger. Note that PixFRET (Feige et al., 2005; Schindelin et al., 2012) corrects for variation in donor and acceptor between data sets as the product of their fluorescence signals. Lowercase letters indicate significance at $P < 0.01$; uppercase letters indicate significance at $P < 0.05$.

interacting partner sets. Analysis of the resulting FRET images showed a strong signal with the SYP121-VAMP721 positive control and a lower, but highly significant, signal when the R-SNARE was paired with EXO70A1, but no appreciable signal between EXO70A1 and VAMP723 or the negative 2xGFP control, despite the comparable levels of donor and acceptor fluorescence (Figure 2). These data support the capacity for EXO70A1 and VAMP721 to interact in planta and are consistent with the mbSUS findings on heterologous expression in yeast.

Impaired Exocyst Function Inhibits Secretion at the Plasma Membrane

To explore the contributions of EXO70A1 subunit to secretory vesicle traffic, we used the tetracistronic expression vector pTecG–2in1–CC (Karnik et al., 2013; Grefen et al., 2015; Zhang et al., 2015). The pTecG–2in1–CC vector incorporates, within a single backbone, expression cassettes for secreted yellow fluorescent protein (secYFP) to monitor traffic, GFP-HDEL as a marker for transformation and for ratiometric quantification of secretion, and two additional cassettes for expressing proteins of interest. Using this vector ensured equal genetic loads for the encoded proteins, enabling the essential controls for quantification of their actions on a cell-by-cell basis, which would not be possible by other means (Grefen and Blatt, 2012). Previous studies showed that blocking secretory traffic yielded a substantial increase in the cellular YFP:GFP fluorescence ratio recorded by confocal fluorescence imaging (Karnik et al., 2013) and concomitant and quantitative loss in secYFP protein collected from the apoplast (Grefen et al., 2015).

We transiently expressed the pTecG–2in1–CC vector with secYFP and GFP-HDEL alone in the wild-type and *exo70A1* Arabidopsis seedling roots to visualize and quantify secretion at the plasma membrane. As a positive control for secretory block, seedlings were transiently transformed with the same vector carrying the cytoplasmic domain of SYP121 ($SYP121^{\Delta C}$) that

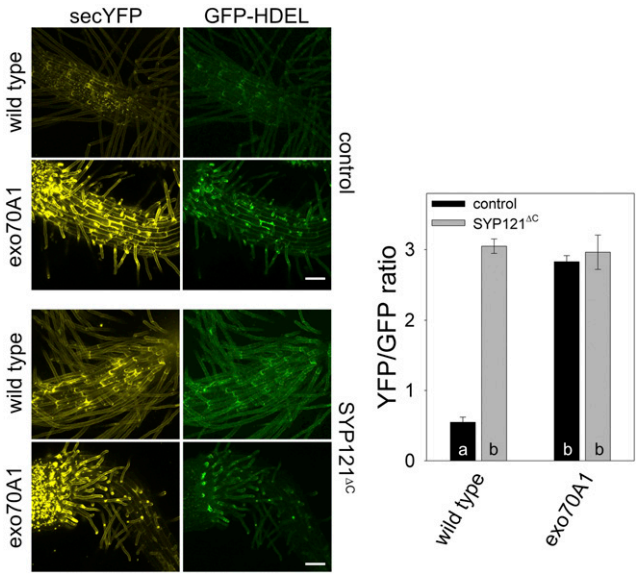

Figure 3. *exo70A1* Mutation Impairs Secretion.

Transient expression of secYFP in the hypocotyl and root of the 5-d-old wild-type and *exo70A1* Arabidopsis seedlings. To ensure equal genetic loads, seedlings were transformed with the pTecG-2in1-CC multicistronic vector (Karnik et al., 2013) carrying cassettes to express secYFP, GFP-HDEL as an expression and ratiometric marker. The lower set of images show the results of including the dominant-negative SYP121$^{\Delta C}$ fragment as a test for secretory block. When expressed with GFP-HDEL alone, secYFP yielded a modest signal relative, consistent with its loss to the medium on secretion (Grefen et al., 2015). When expressed additionally with SYP121$^{\Delta C}$ an increase in secYFP signal relative to GFP-HDEL was evident, indicating secretory block and secYFP retention in the tissue (Tyrrell et al., 2007; Grefen et al., 2015). Note the retention of secYFP in the *exo70A1* mutant, even in the absence of SYP121$^{\Delta C}$ expression. YFP-to-GFP fluorescence ratios calculated after subtracting the autofluorescence signals from untransformed seedlings. Data are means ± SE, each of $n \geq 18$ independent transformants, with letters indicating statistical significance on post hoc Holm-Sidak analysis ($P < 0.001$). Bar = 50 μm.

functions as a dominant-negative fragment and suppresses secretion at the plasma membrane (Tyrrell et al., 2007; Grefen et al., 2015). Expressing SYP121$^{\Delta C}$ in the wild-type and *exo70A1* mutant seedlings provided a basis for comparing the impact on secretion in each genetic background.

We quantified a secretory block as the ratio of YFP-to-GFP fluorescence in live imaging of the transiently transformed seedlings by confocal microscopy (Figure 3). In the absence of SYP121$^{\Delta C}$, we observed a significant block of secretion in the *exo70A1* mutant compared with the wild-type seedlings, evidenced by the elevated mean in the YFP:GFP ratio. Seedlings transformed to express the SYP121$^{\Delta C}$ fragment in addition to the fluorescent proteins yielded a similar mean YFP:GFP ratio in the *exo70A1* mutant. By contrast, the mean YFP:GFP ratio was statistically different and much higher on expressing the SYP121$^{\Delta C}$ fragment in the wild type than in its absence. These results showed that the impaired exocyst function in the *exo70A1* mutant inhibits secretion to the plasma membrane with an efficacy comparable with that of the SYP121$^{\Delta C}$ fragment. Furthermore, given the absence of further secretory suppression in the presence of the SYP121$^{\Delta C}$ fragment, the results suggest that this inhibition functionally overlaps with that introduced by the Qa-SNARE fragment.

SNARE Protein Localization Is Altered in the exo70A1 Mutant

Both the exocyst and a subset of SNARE proteins associate dynamically with the plasma membrane. The exocyst forms a peripheral membrane complex (Fendrych et al., 2013; Synek et al., 2014; Kulich et al., 2018). The Qa- and R-SNAREs are integral membrane proteins; whereas SYP121 localizes to the plasma membrane (Lipka et al., 2007; Honsbein et al., 2009; Grefen et al., 2015; Waghmare et al., 2019), the R-SNAREs, including VAMP721, localize to the vesicle membrane and associate transiently with the plasma membrane (Uemura et al., 2005; Zhang et al., 2011, 2015). We therefore asked whether the loss of one interacting partner could affect the localization of the other as a possible mechanism to explain secretory block.

For this purpose, SNARE and exocyst GFP protein fusion constructs were stably transformed into the reciprocal exocyst and SNARE mutant backgrounds. We quantified their distributions as ratios between the fluorescence signal present at the cell periphery, delineated as the first 2 μm from the cell surface, and in the interior of cells within the hypocotyl and roots of transgenic plants, normalizing the fluorescence distribution to the total fluorescence signal in each case. In the *exo70A1* mutant, we observed a pronounced shift in VAMP721-GFP away from the cell periphery (Figures 4A and 4C), much as has been reported also for the *sec84b* exocyst mutant (Fendrych et al., 2013). Similarly, VAMP722-GFP and SYP121-GFP distributions were reduced at the cell periphery in *exo70A1* mutants compared with the wild type (Figures 4A and 4B). However, the GFP-EXO70A1 signal, which localized primarily to the cell periphery, was not significantly affected in each of the SNARE mutant backgrounds (Figures 4C and 4D). These results suggest that EXO70A1 is important either for localization of the SNAREs or their maintenance at the cell periphery, especially of the R-SNAREs. This interpretation is consistent with the idea that EXO70A1 is important for exocyst targeting (Fendrych et al., 2013; Kalmbach et al., 2017) and its loss delocalizes and destabilizes the exocyst complex, thereby affecting SNARE complex assembly, SNARE protein delivery, or SNARE recycling. The interpretation is also supported by evidence from yeast that suggests exocyst subunits can bind both vesicle- and plasma membrane–associated proteins (Shen et al., 2013; Yue et al., 2017; Mei and Guo, 2019; Rossi et al., 2020).

Differential Effects of Exocyst–SNARE Interactions on Plant Growth

Single mutants of several plasma membrane SNAREs normally show subtle defects in Arabidopsis; these weak phenotypes are generally thought to reflect functional redundancies. For example, the single R-SNARE mutants *vamp721* and *vamp722* are largely indistinguishable from the wild type and only the double *vamp721vamp722* mutant is lethal (Zhang et al., 2011). Similarly,

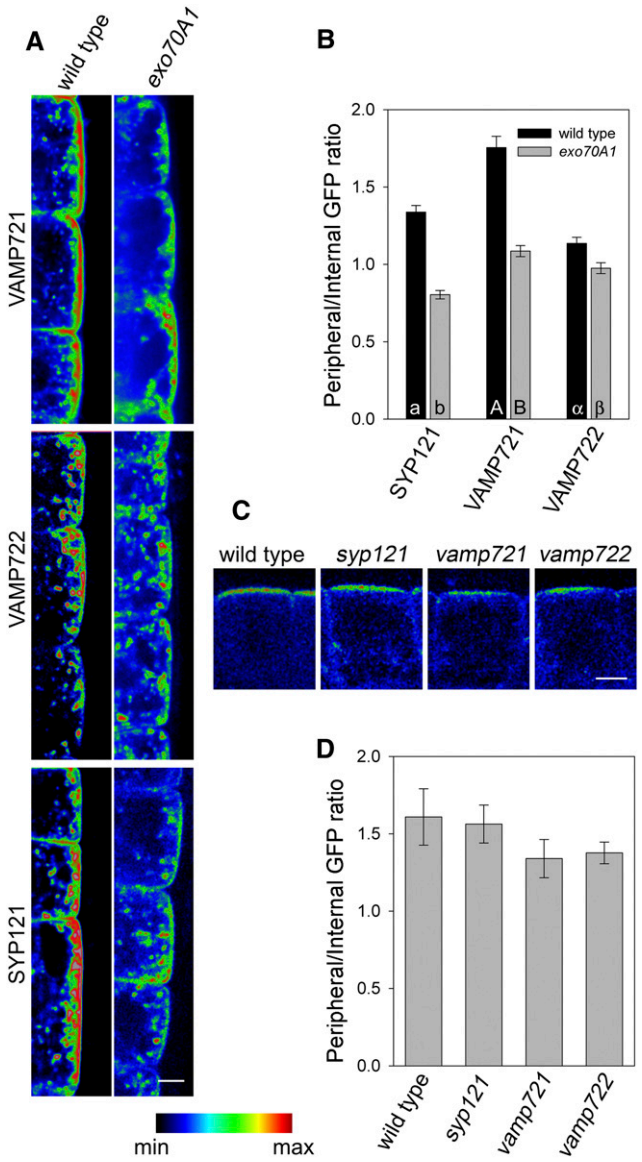

Figure 4. SNARE Localization Is Affected in the *exo70A1* Mutant.

(A) Representative images of VAMP721, VAMP722, and SYP121 localized as GFP fusions in the wild-type and *exo70A1* mutant Arabidopsis, showing a redistribution of the SNAREs in the exocyst mutant.

(B) SYP121, VAMP721, and VAMP722 localization in the wild-type (black) and *exo70A1* mutant (gray) Arabidopsis, including data in **(A)**, as the ratio of fluorescence between the periphery and cytosol, indicating a shift of SNARE distribution to the cytosol in the absence of EXO70A1. Data are means ± SE, each of $n \geq 36$ randomly selected images from $n \geq 6$ independent experiments, with letters indicating pairwise statistical significance from post hoc Holm-Sidak analysis ($P < 0.001$).

(C) Representative images of GFP-tagged EXO70A1 in the wild-type and *syp121*, *vamp721*, and *vamp722* mutant Arabidopsis, showing no appreciable change in its peripheral localization.

(D) EXO70A1 localization in the wild-type and *syp121*, *vamp721*, and *vamp722* mutant Arabidopsis as the ratio of fluorescence between the periphery and cytosol. Data are means ± SE, each of $n \geq 36$ randomly selected images from $n \geq 6$ independent experiments. No statistically significant differences from the wild type were evident. Bars in **(A)** and **(C)** = 10 μm.

the single Qa-SNARE mutants *syp121* and *syp122* exhibit strong phenotypes that surface only when challenged with abiotic and biotic stress (Zhang et al., 2008; Eisenach et al., 2012; Waghmare et al., 2018), again reflecting functional overlaps as well as potential specificities among noncanonical protein partners. The single mutant *exo70A1* also exhibits a range of phenotypes, including reduced vegetative growth and cell-specific patterning (Synek et al., 2006; Fendrych et al., 2010; Kalmbach et al., 2017; Vukašinović et al., 2017). These characteristics are consistent with the effects of the *exo70A1* mutant in secretory traffic and SNARE localization, despite the apparent lack of any additive effect over that of the SYP121$^{\Delta C}$ dominant-negative fragment (Figures 3 and 4).

Vesicle tethering by the exocyst is thought to occur before the SNAREs assemble to drive vesicle fusion, but both are necessary for cargo secretion (Bassham and Blatt, 2008; Ravikumar et al., 2017). We therefore hypothesized that loss of both *EXO70A1* and single SNARE gene expression should exhibit defects synergistic to those of the single mutant parents if the functions of the gene products are closely connected. The *exo70A1* null mutant is male lethal and is impaired in stigma receptivity (Synek et al., 2006). Therefore, we crossed *exo70A1*$^{+/-}$ heterozygote with the homozygotic mutants *vamp721*$^{-/-}$ and *syp121*$^{-/-}$ and examined the segregation of the double mutant in the F2 generations. Growth of the *syp121* mutant is normally only marginally retarded compared with the wild type (Bassham and Blatt, 2008; Eisenach et al., 2012). Like the *exo70A1* single mutant, we found that growth of the double *exo70A1 syp121* mutant showed a significant but modest reduction in vegetative growth in the F2 generation, suggesting that the *exo70A1* mutation is epistatic to that of *syp121*.

By contrast, the F2 population of the *exo70A1*$^{+/-}$ and *vamp721*$^{-/-}$ cross yielded a segregating population of extremely dwarfed plants, each of which was identified as a *exo70A1 vamp721* double mutant (Figures 5A and 5B). The *exo70A1 vamp721* double mutant plants could be maintained for up to 10 weeks when grown under a short-day light cycle, but the plants remained severely dwarfed, showed late lethality, and failed to flower. We therefore maintained the double mutant as a *exo70A1*$^{+/-}$*vamp721*$^{-/-}$ segregating population.

To examine the mutant lines in greater detail, we grew seedlings on agar plates for 10 d and examined the characteristics of early development following germination. The *exo70A1 vamp721* double mutants showed severely stunted growth in the root and cotyledon expansion was much reduced compared with the wild-type seedlings and the single mutant parents (Figure 5C). These phenotypes were evident 7 to 10 d after germination. Transient transformation by cocultivation must be started with younger seedlings, precluding direct assays of traffic using the pTecG–2 in1–CC vector with secYFP and GFP-HDEL (Figure 3). Nonetheless, we noted that the *exo70A1 vamp721* double mutants produced small, delicate leaves with morphologically similar structure. Quantitative analysis of the epidermal cells, which are important drivers in leaf expansion (Walter et al., 2009), showed that in the *exo70A1 vamp721* double mutants these cells were significantly smaller than those from leaves of the wild-type and single mutant plants (Figures 5D and 5E). These observations are consistent with suppressed cell expansion arising from the

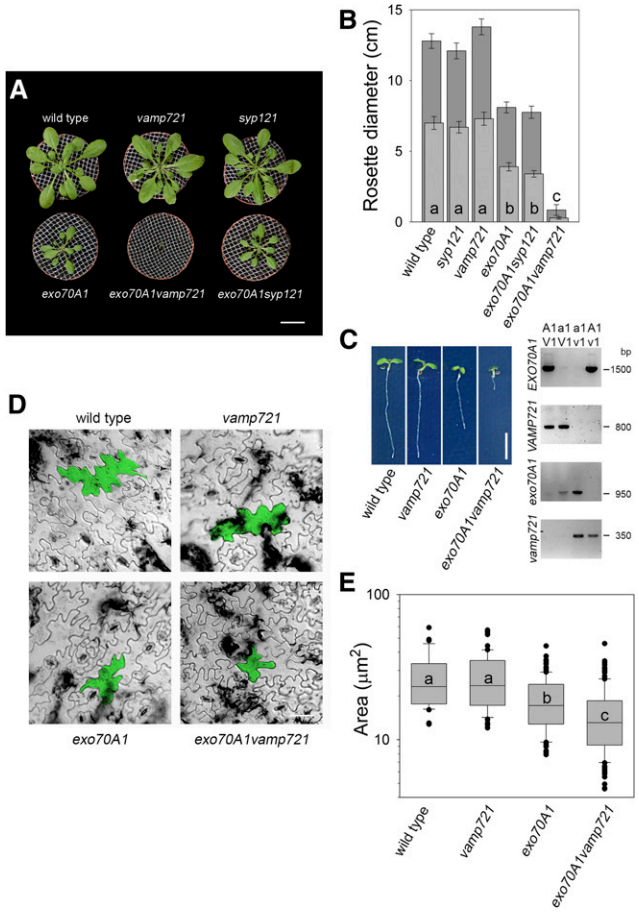

Figure 5. *exo70A1 vamp721* Double Mutant Synergistically Suppresses Growth.

(A) Representative Arabidopsis plants grown over 4 weeks under 16-h-light/8-h-dark from F2 seed germinated on soil to isolate the double mutants from crosses of the SNARE mutants with *exo70A1*. *syp121* and *vamp721* single mutants were visually indistinguishable from the wild type, while the *exo70A1* mutant was 40 to 50% smaller than the wild type. *exo70A1 syp121* double mutants were visually indistinguishable from the *exo70A1* single mutant, while the *exo70A1 vamp721* double mutant showed a severe suppression of growth unique from the wild-type and single mutant parents. Plants in every case were genotyped as in **(C)**. Bar = 2 cm.

(B) Rosette diameter of Arabidopsis grown over 4 (light gray bars) and 8 weeks (dark gray bars) as in **(A)**. Data are means ± SE of $n \geq 10$ plants for each line. Letters indicate significant differences with post hoc Holm-Sidak analysis ($P < 0.01$).

(C) (Left) Seedling and root development of the wild type, *exo70a1* and *vamp721* single mutants, and *exo70a1 vamp721* double mutants grown on 0.5 MS and 1% agar medium for 10 d. Note the modest reduction in growth and smaller epinastic cotyledons of the *exo70A1* mutant and much stronger growth suppression of the *exo70A1 vamp721* double mutant. (Right) Seedling genotypes confirmed by PCR using gene-specific primers (Supplemental Table) and a T-DNA left boarder primer to amplify the wild-type and mutant allele products. V1 and A1 indicate the wild-type alleles of *VAMP721* and *EXO70A1*, respectively; v1 and a1 indicate the T-DNA mutant alleles of *vamp721* and *exo70A1*, respectively. Bar = 1 cm.

(D) and **(E)** Epidermal cell size analysis of mature leaves of 8-week-old plants of single and double mutant Arabidopsis. Leaf epidermal peels **(D)** were analyzed for epidermal cell surface area (green) and data assembled **(E)** in a box and whisker plot. Cell area of *exo70a1 vamp721* plants were significantly smaller than those of the wild-type and parental lines. Data are means ± SE of $n \geq 150$ cells chosen at random from $n \geq 8$ plants for each line. Note the logarithmic *y* axis scale. Letters indicate significant differences with post hoc Holm-Sidak analysis ($P < 0.001$). Bar = 50 μm.

impaired traffic of the *exo70A1 vamp721* double mutant, and they implicate specific overlaps in the progression of exocyst–SNARE interactions that occur in the events leading up to secretion.

DISCUSSION

Models of exocytosis have generally divided the process into three stages, vesicle tethering, docking, and fusion, each thought to occur as part of a serial progression with distinct sets of proteins that regulate each step (Cai et al., 2007; Bassham and Blatt, 2008; Zarský et al., 2009). Major protein assemblies contributing to this progression include exocyst and SNARE complexes, each of which relies on interactions between a discrete set of protein subunits and on their correct cellular location for function. Even so, there is growing evidence that these assemblies are not isolated interaction networks (Shen et al., 2013; Mei and Guo, 2019; Rossi et al., 2020) nor, as we now show, are their functional impacts. Here, we present evidence in vitro and in vivo that point to direct interactions in Arabidopsis between members of the exocyst complex EXO70 subunit family that are important for vesicle tethering and recruitment to the plasma membrane, and the SNAREs that drive the final stages of membrane fusion. Furthermore, the functional bias evident among these interactions leads to a clear hierarchy between exocyst–SNARE binding partners with differential consequences for SNARE protein localization, secretion, cellular expansion, and vegetative growth. Thus, our findings point both to an overlap between the exocyst and SNAREs and to a temporal "handshake" between subunits of these protein complexes that is necessary for vesicles to progress through the final stages of tethering and fusion.

Exocyst–R-SNARE Interactions Engender a Functional Synergy in Membrane Traffic

A singular feature of the EXO70-SNARE interactions we uncovered through yeast mbSUS is its R-SNARE bias. Each of the major plasma membrane-associated SNAREs—the Qa-SNARE SYP121; the R-SNAREs VAMP721, VAMP722, VAMP724, and VAMP727; and to lesser extents, the Qa-SNARE SYP122 and Qbc-SNARE SNAP33—bound differentially with several EXO70 subunits, but not with the endomembrane R-SNARE VAMP723 (Figure 1; Supplemental Figure 1). These data also highlighted an overall pattern among the EXO70 subunits that favored the plasma membrane R-SNAREs, as demonstrated by VAMP721. In secretory traffic assays, we found no evidence for an additional impact of the cognate Qa-SNARE SYP121 in secretory trafficking assays (Figure 3) when combined with the *exo70a1* mutant. The block of traffic in the the *exo70a1* mutant was comparable with that of the dominant-negative SYP121$^{\Delta C}$ fragment that competes with the full-length Qa-SNAREs SYP121 and SYP122 to suppress

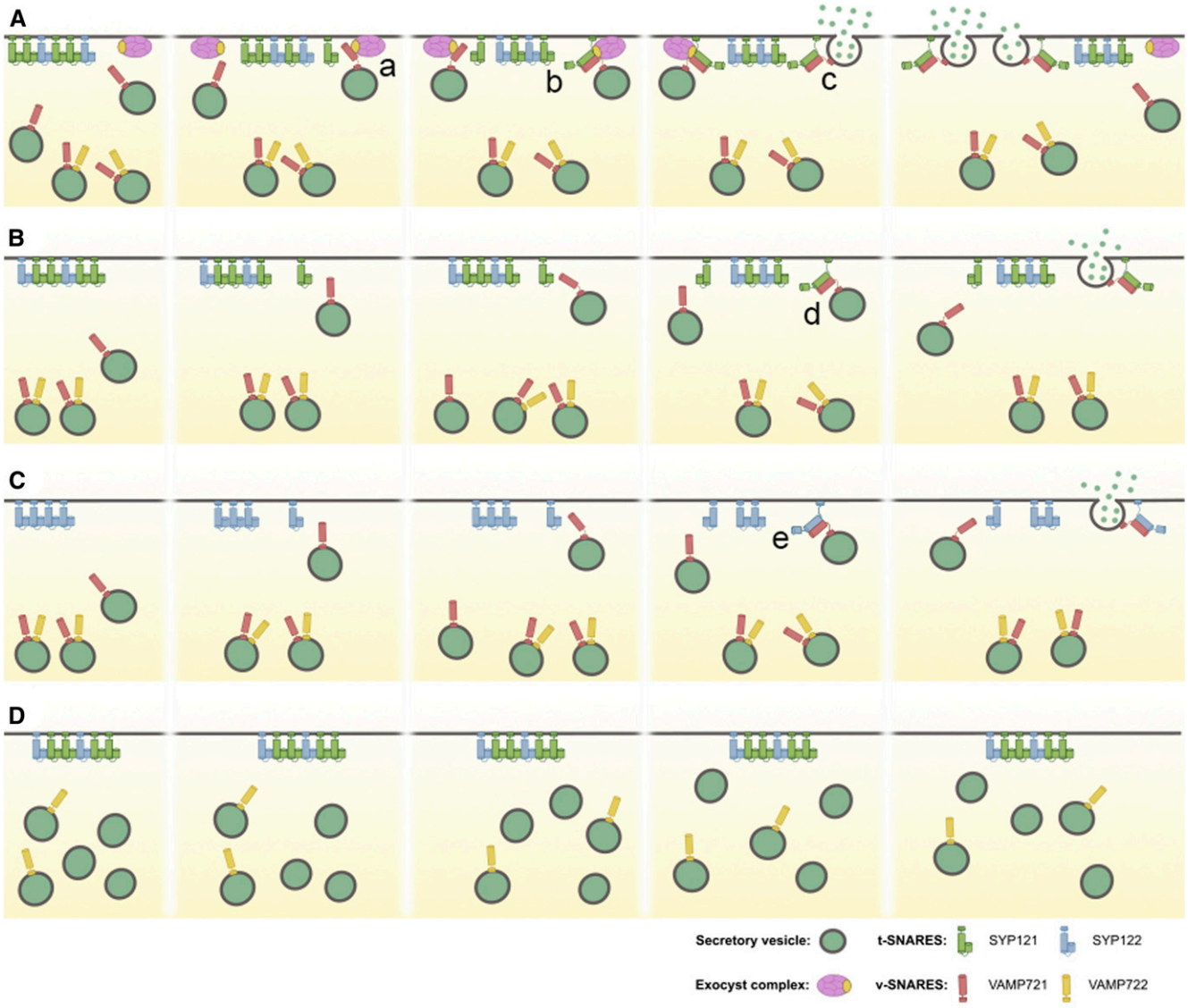

Figure 6. Model of Exocyst and R-SNARE Binding in Sequential Recruitment and SNARE Complex Assembly for Secretion.

Cartoon of EXO70A1 and VAMP721 synergy in vesicle fusion. Peripherally localized EXO70A1 is indicated by the exposed (orange) face of an oval exocyst complex (purple). SYP121 and SYP122 are shown in green and blue, respectively, with membrane anchor, longer H3 (SNARE) and shorter Habc domains. VAMP721 and VAMP722 are shown in red and yellow, respectively, with only a membrane anchor and SNARE domain. Other SNARE and associated proteins are omitted for clarity.

(A) Normal (wild-type) secretion engages EXO70A1 in sequentially recruiting VAMP721 (a) and SYP121 from Qa-SNARE "icebergs" (b) leading to vesicle fusion (c).

(B) *exo70a1* mutant impairs secretion by slowing trans-SNARE assembly (d).

(C) *exo70a1 syp121* double mutant similarly slows secretion with the remaining excess of Qa-SNARE SYP122 available for trans-SNARE assembly (e).

(D) *exo70a1 vamp721* double mutant strongly suppresses secretion by reducing R-SNARE availability as well as eliminating exocyst recruitment for trans-SNARE assembly.

secretion (Tyrrell et al., 2007; Grefen et al., 2015), and their combination yielded no evidence of additive interaction. Similarly, the strongest effect in complementary protein localization assays was of the *exo70a1* mutant on VAMP721 (Figure 4).

Most telling, however, we uncovered a functional synergy of EXO70A1 with the R-SNARE. Crossings to yield the *exo70a1 syp121* double mutant resulted in mutant plants with characteristics similar to the effects of the *exo70a1* mutant; by contrast, the *exo70a1 vamp721* double mutant was strongly impaired in cell expansion, exhibited severe dwarfing in vegetative growth, and failed to transit to flowering, even though the *vamp721* mutant showed no impact on cell expansion or vegetative growth

(Figure 5; Zhang et al., 2011, 2015, 2017). The effects of EXO70A1 with the Qa-SNARE can be understood as the result of the sequential actions of the exocyst and Qa-SNARE, so that the exocyst subunit mutation dominates over events engaging the Qa-SNARE. Such is not true for the effects of the EXO70 subunit mutation with that of the R-SNARE. In this case, the strong synergy evident in vivo is best understood in context of a mutual interdependence in the roles of the two proteins. Most important, this synergy implies a clear hierarchy among interactions between the Qa-SNARE SYP121 and the R-SNARE VAMP721 with EXO70A1.

How is the spatiotemporal overlap of EXO70 and R-SNARE binding enfolded within the respective roles of these subunits within the functions of their respective complexes? In vivo and cryo-electron microscopy analyses of the exocyst complex indicate a topologically optimal space between the exocyst complex, plasma membrane, and tethered vesicle membrane in yeast that could accommodate exocyst and SNARE proteins in association (Picco et al., 2017; Mei et al., 2018). This proximity of exocyst and SNARE complexes fits well with the evidence of direct physical interaction, the requirement for EXO70A1 in SNARE distributions (Figures 2 and 4), and with previous evidence for a close complementarity in protein localizations in yeast and plants (Fendrych et al., 2013; Shen et al., 2013). The exocyst topology suggests that the EXO70 subunit is exposed to the cytosol when the exocyst complex is anchored to the plasma membrane. Such exposure would certainly offer a surface for interaction with the R-SNARE and its cytosolic longin domain as the vesicle membrane approaches its target. Indeed, recent findings implicate vesicle tethering in yeast that depends on R-SNARE binding with Sec6 associated in complex with EXO70: Rossi et al. (2020) developed an in vitro assay using vesicle clustering to monitor tethering, incorporating components of the exocyst, to show that clustering is enhanced by the vesicle-localized R-SNARE Snc2 and strongly promoted with EXO70 mutants that bypass Rho GTPase activation. These results, and reconstructions from single-particle electron microscopy, indicate a conformational change of the holocomplex on activation by the Rho GTPase that exposes a binding site within the Sec6-EXO70 complex for the R-SNARE. Although interactions in yeast between the R-SNARE and exocyst appear dominated by binding to the exocyst Sec6 subunit, in vitro assays have indicated a direct interaction between the EXO70 subunit and Snc2 (Shen et al., 2013). Assuming similar topological relationships for Arabidopsis, the functional synergy uncovered for EXO70A1 and VAMP721 leads us to posit that these binding events precede SYP121 introduction and the assembly of VAMP721 with the Qa-SNARE leading to vesicle fusion.

EXO70 and SNARE Redundancies

It is perhaps surprising that, unlike the parental *exo70A1* and *vamp721* mutants, the *exo70A1 vamp721* double mutant exhibited so profound a set of phenotypes allied to secretory traffic. The EXO70 subfamily in Arabidopsis incorporates 23 members and although the majority of these differ in developmental and tissue-specific expression, there are nonetheless overlaps (Cvrčková et al., 2012). Similarly, VAMP721 and VAMP722 are near sequence identical, and with the exception of the associated interactions with the Sec1/Munc18 protein SEC11 that distinguish their binding between the plasma membrane Qa-SNAREs SYP121 and SYP122 (Karnik et al., 2015), the two R-SNAREs appear functionally redundant. Nonetheless, the several plasma membrane Qa- and R-SNAREs, although cross-interactive and seemingly redundant in function, show very different phenotypes. Consider SYP121 and SYP122 that both bind the R-SNAREs VAMP721 and VAMP722. The single *syp121* and *syp122* mutant plants appear similar to the wild type when grown under permissive conditions (Zhang et al., 2007), and the dominant-negative SYP121$^{\Delta C}$ and SYP122$^{\Delta C}$ fragments are equally effective in secretory traffic block in vivo (Tyrrell et al., 2007; Grefen et al., 2015). Yet, the two Qa-SNARE null mutants show very different phenotypes in pathogen defense and abiotic stress resistance (Collins et al., 2003; Zhang et al., 2007; Eisenach et al., 2012) and the Qa-SNAREs mediate the traffic of different subsets of secretory cargo (Rehman et al., 2008; Waghmare et al., 2018). These, and associated studies (Reichardt et al., 2011; Hashimoto-Sugimoto et al., 2013; Xia et al., 2019; Zhang et al., 2019), implicate a functional network of trafficking and related regulatory protein partners that is substantially more dynamic than may be deduced from an analysis of gene families.

Our present data do not speak directly to the functional specificities among the several plasma membrane SNAREs with EXO70A1. Even so, when compared with VAMP722, we note that the peripheral localization of VAMP721 was most strongly affected in the *exo70a1* mutant (Figure 4), which may indicate more subtle functional differences between the two R-SNAREs that have yet to be resolved. Furthermore, the strong phenotypic synergy in the *exo70A1 vamp721* double mutant that we identified indicates that the presence of VAMP722 is not sufficient to compensate for the loss of VAMP721. One simple explanation is that EXO70A1 and VAMP721 may be specialized as a functional unit, analogous to that implicated in yeast (Shen et al., 2013; Rossi et al., 2020), for the delivery of a unique set of cargos critical to the growth of the plant, much as is now evident from analysis of the distribution of cargos between the Qa-SNAREs SYP121 and SYP122 (Waghmare et al., 2018).

Finally, our data focus attention to the longin domain of the R-SNARE. The longin domain of VAMP721 was previously shown to be a key regulator in SNARE protein interactions (Uemura et al., 2005). It is essential for selective binding with noncanonical K^+ channel partners that have been suggested to coordinate secretion with K^+ uptake (Zhang et al., 2015) and, as we demonstrate, it is important for the interactions with several EXO70 subunits (Figure 1; Supplemental Figures 1 and 3). Thus, the VAMP721 longin domain may function as the nexus in a progression of hand-offs between multiple binding partners. We speculate that the exocyst complex could participate in targeting VAMP721-loaded vesicles to the plasma membrane through direct interactions between SNAREs and the exocyst during vesicle tethering and/or recruitment to the plasma membrane (Figure 6). Important questions now will be to identify the domains within the plant EXO70 and SNARE proteins that are critical for their interactions and to determine their dynamics in context of vesicle delivery to the plasma membrane.

METHODS

Plant Growth Conditions, Crosses, and Genotyping

Seeds from the wild-type (Columbia-0) and mutant Arabidopsis (*Arabidopsis thaliana*) were stratified in the dark at 4°C and then germinated in long-day conditions in growth chambers (60% relative humidity, 16-h-light/8-h-dark cycle, 22°C) on half-strength Murashige and Skoog (MS) medium solidified with 1% (w/v) agar. Sealed plates were placed in long-day light conditions (150 μmol m^{-2} s^{-1} photosynthetically active radiation) before seedlings were evaluated for mutant phenotypes and collected for genotyping or were transplanted to single pots or 15-holder trays for further growth and observation.

To generate the *exo70A1 vamp721* double mutant, the heterozygous *exo70A1*$^{+/-}$ (SALK_135462) mutant was used as a maternal parent in a cross with the homozygous *vamp721* mutant (SALK_037273). The F1 generation was allowed to self-fertilize, and the F2 seed was collected for further analysis. Tissue was harvested from individual F1 and F2 plants of the *ex70A1*$^{+/-}$ $\times$ *vamp721* cross for PCR analysis using gene-specific and T-DNA primers (Supplemental Table). Double heterozygous F1 mutants were identified and allowed to set seed. Since the *exo70A1* single mutant is infertile, a segregating population of *exo70A1*$^{+/-}$*vamp721*$^{-/-}$ was maintained for isolating double mutants. For the *exo70A1 syp121* double mutant, the *exo70A1*$^{+/-}$ (SALK_135462) line was crossed with the *syp121* null mutant carrying a point mutation that encodes a premature stop codon and does not produce a transcript but introduces a *Mlu*I restriction site that is identifiable as a band shift on digestion (Pajonk et al., 2008).The double mutant was propagated as an *exo70A1*$^{+/-}$*syp121*$^{-/-}$ line.

Yeast and Plant Vector Construction

All plasmids were constructed using the Gateway cloning system (Thermo Fisher Scientific). Details for all yeast and plant expression vectors are included in publications as cited in the text and can be found at www.psrg.org.uk.

mbSUS

Haploid yeast strains for bait and prey, THY.AP4 and THY.AP5, respectively, were used to express pMetYOst-Dest or pNX35-Dest constructs of exocyst subunits or SNARE proteins and analyze protein–protein interactions as described previously (Zhang et al., 2017). Ten to 15 yeast colonies were selected and inoculated into selective media (CSM_{-LM} for THY.AP4 and CSM_{-MTU} for THY.AP5) for overnight growth at 180 rpm and 28°C. Liquid cultures were harvested and resuspended in yeast extract peptone dextrose (YPD) medium. Yeast mating was performed in sterile PCR tubes by mixing equal aliquots of yeast containing bait and prey construct. Aliquots of 5 μL were dropped on YPD plates and incubated at 28°C overnight. Colonies were transferred from YPD onto CSM_{-LTUM} plates and incubated at 28°C for 2 to 3 d. Diploid colonies were selected and inoculated in liquid CSM_{-LTUM} media and grown at 180 rpm 28°C overnight before harvesting by centrifugation and resuspension in sterile water. Serial dilutions at OD_{600} 1.0 and 0.1 in water were dropped, 5 μL per spot, on $CSM_{-LTUMAH}$ plates with added Met. Plates were incubated at 28°C, and images were taken after 3 d. Yeast were also dropped on CSM_{-LTUM} control plates to confirm mating efficiency and cell density, and growth was imaged after 24 h at 28°C. To confirm construct expression, mated yeast was grown overnight in 5 mL of selective medium and harvested by centrifugation at 5000*g*. Pelleted yeast was resuspended in diluted lysis buffer (1/1 [v/v], 10% SDS, 4 mM EDTA, 0.2% Triton-X 100, 0.01% bromophenol blue, 20 mM DTT, 20% glycerol, and 100 mM Tris, pH 6.8), sonicated two times for 30 s, and boiled at 100°C for 5 min. Prepared protein samples were loaded on 10% polyacrylamide gels and blotted onto a nitrocellulose membrane. The membrane was blocked overnight (1$\times$ PBS, 0.25% [v/v] Tween, and 5% [w/v] low fat milk) and then incubated with primary α-HA or α-VP16 antibodies at 1:2000 dilution. Proteins were detected using the secondary α-mouse or α-rabbit antibodies (Promega).

Transformations for FRET and Secretion Analysis

Nicotiana benthamiana plants with fully expanded true leaves were used for transient transformation with *Agrobacterium tumefaciens* strain GV3101 carrying the multicistronic vector pFRETgc-2in1-NN that enabled simultaneous expression of GFP and mCherry protein fusions (Hecker et al., 2015). Overnight cultures of GV3101 expressing these constructs were diluted in infiltration buffer (10 mM $MgCl_2$ and 100 μM acetosyringone) to OD_{600} 0.07 and infiltrated with a syringe into the abaxial surface of *N. benthamiana* leaves. A Zeiss LSM 880 confocal microscope with 40$\times$ water immersion objective (Zeiss) was used for image acquisition of transformed *N. benthamiana* leaves. For FRET, the GFP constructs were excited at 488 nm and detected at 505 to 530 nm. mCherry constructs were detected at 600 to 620 nm after excitation at 552 nm to assess fluorophore expression and at 488 nm to collect the FRET signal. FRET image analysis was performed using the PixFRET tool (Feige et al., 2005) in ImageJ (Schindelin et al., 2012) applied to image stacks across the entire fields of view. PixFRET corrects for spectral bleed-through and for variations in donor and acceptor signals using the product of their fluorescence signals on a pixel-by-pixel basis. FRET analysis of each experiment was typically applied to three to five randomly selected images for each construct pair.

Secretion assays used the tetracistronic vector pTecG-2in1-CC (Karnik et al., 2013) that incorporates four expression cassettes, each driven by a 35S promoter, two carrying the coding sequences for secYFP and GFP-HDEL, and the remaining two cassettes providing Gateway recombination sites for proteins of interest. Assays were performed without and with $SYP121^{\Delta C}$ incorporated in one of the latter cassettes as described previously (Karnik et al., 2013). Arabidopsis seed was sterilized and grown in 0.05 MS liquid medium for 2 to 3 d until root and cotyledons emerged. Seedlings were then cocultivated with Agrobacterium carrying the multicistronic constructs for an additional 3 to 4 d before imaging. Live root epidermal tissue was imaged under a SP8-SMD confocal microscope with a 20$\times$/0.85 numerical aperture objective (Leica Microsystems) using the 470-nm and 514-nm laser lines for excitation and fluorescence was collected over the bandwidths 490 to 530 and 520 to 565 nm for the GFP and YFP protein fusions, respectively. Roots and roothairs were routinely assayed near the root base to ensure imaging of live cells, and cell viability was checked by monitoring of cytoplasmic streaming in root hairs. GFP and YFP signals were corrected for background postcollection using the mean signals from untransformed seedlings before calculating YFP:GFP fluorescence ratios.

Protein Localization

The dynamic study of the lateral membranes of root epidermal cells of the elongation zone was performed on a Nikon TE200e with a Yokogawa Andor spinning disc unit with 40$\times$ and 63$\times$ oil immersion objectives. The images were processed by Fiji/ImageJ software, and the periphery:internal ratio was calculated as previously described after demarking a 2-μm-wide perimeter at the cell surface corresponding to the peripheral zone (Fendrych et al., 2010).

Statistics

Statistical analyses were conducted with the SigmaPlot (Systat Software) utility for analysis of variance with post hoc Holm-Sidak analysis.

Accession Numbers

Genes used in this study can be found in The Arabidopsis Information Resource (www.arabidopsis.org) under the following identifiers: SYP121

(At3g11820); VAMP721 (At1g04750); VAMP723 (At2g33110); EXO70A1 (At5g03540).

Supplemental Data

Supplemental Figure 1. EXO70 homologs interact differentially with several SNAREs.

Supplemental Figure 2. Immunoblot analysis for EXO70 interaction with several SNAREs.

Supplemental Figure 3. The longin domain of VAMP721 is essential for EXO70 interaction.

Supplemental Figure 4. Immunoblot analysis for EXO70 interaction with VAMP721, VAMP723 and their chimeras.

Supplemental Table. Gene-specific primers for PCR analysis of parental lines and crosses.

ACKNOWLEDGMENTS

We thank Jana Šťovíčková (Laboratory of Cell Biology, Institute of Experimental Botany of the Czech Academy of Sciences) for technical help with plant harvesting, and Martin Potocký and Tamara Pečenková for critical reading of this article. This work was supported by the Ministry of Education, Youth and Sports of the Czech Republic from the European Regional Development Fund-Project "Centre for Experimental Plant Biology" (grant CZ.02.1.01/0.0/0.0/16_019/0000738), the Imaging Facility of the Institute of Experimental Botany of the Czech Academy of Sciences and Ministry of Education, Youth and Sports of the Czech Republic (grants LM2018129 Czech-BioImaging, OPVVV455 CZ.02.1.01/0.0/0.0/16_013/0001775, and OPPK CZ.2.16/3.1.00/21519), the Biotechnology and Biological Science Research Council (grants BB/L019025/1, BB/N006909/1, BB/P011586/1, and BB/N01832X/1), and the Royal Society (grant IE150953 to M.R.B.).

AUTHOR CONTRIBUTIONS

M.R.B., V.Ž., E.R.L., and J.O. developed the project; E.R.L. and J.O. designed the experiments; E.R.L., J.O., and N.A.D. performed the experiments; E.R.L., J.O., J.A., and M.R.B. analyzed and interpreted the data; E.R.L. and J.O. wrote the article with M.R.B. and V.Ž.

Received April 20, 2020; revised June 23, 2020; accepted July 20, 2020; published July 22, 2020.

REFERENCES

Bassham, D.C., and Blatt, M.R. (2008). SNAREs: Cogs and coordinators in signaling and development. Plant Physiol. **147:** 1504–1515.

Blatt, M.R., and Thiel, G. (2003). SNARE components and mechanisms of exocytosis in plants. In The Golgi Apparatus and the Plant Secretory Pathway, D.G. Robinson, ed (Oxford: Blackwell Publishing - CRC Press), pp. 208–237.

Cai, H., Reinisch, K., and Ferro-Novick, S. (2007). Coats, tethers, Rabs, and SNAREs work together to mediate the intracellular destination of a transport vesicle. Dev. Cell **12:** 671–682.

Collins, N.C., Thordal-Christensen, H., Lipka, V., Bau, S., Kombrink, E., Qiu, J.L., Hückelhoven, R., Stein, M., Freialdenhoven, A., Somerville, S.C., and Schulze-Lefert, P. (2003). SNARE-protein-mediated disease resistance at the plant cell wall. Nature **425:** 973–977.

Cvrčková, F., Grunt, M., Bezvoda, R., Hála, M., Kulich, I., Rawat, A., and Zárský, V. (2012). Evolution of the land plant exocyst complexes. Front. Plant Sci. **3:** 159.

Eisenach, C., Chen, Z.H., Grefen, C., and Blatt, M.R. (2012). The trafficking protein SYP121 of Arabidopsis connects programmed stomatal closure and K^+ channel activity with vegetative growth. Plant J. **69:** 241–251.

Fasshauer, D., Sutton, R.B., Brunger, A.T., and Jahn, R. (1998). Conserved structural features of the synaptic fusion complex: SNARE proteins reclassified as Q- and R-SNAREs. Proc. Natl. Acad. Sci. USA **95:** 15781–15786.

Feige, J.N., Sage, D., Wahli, W., Desvergne, B., and Gelman, L. (2005). PixFRET, an ImageJ plug-in for FRET calculation that can accommodate variations in spectral bleed-throughs. Microsc. Res. Tech. **68:** 51–58.

Fendrych, M., Synek, L., Pecenková, T., Drdová, E.J., Sekeres, J., de Rycke, R., Nowack, M.K., and Zársky, V. (2013). Visualization of the exocyst complex dynamics at the plasma membrane of *Arabidopsis thaliana*. Mol. Biol. Cell **24:** 510–520.

Fendrych, M., Synek, L., Pecenková, T., Toupalová, H., Cole, R., Drdová, E., Nebesárová, J., Sedinová, M., Hála, M., Fowler, J.E., and Zársky, V. (2010). The Arabidopsis exocyst complex is involved in cytokinesis and cell plate maturation. Plant Cell **22:** 3053–3065.

Geelen, D., Leyman, B., Batoko, H., Di Sansebastiano, G.P., Moore, I., and Blatt, M.R. (2002). The abscisic acid-related SNARE homolog NtSyr1 contributes to secretion and growth: Evidence from competition with its cytosolic domain. Plant Cell **14:** 387–406.

Grefen, C., and Blatt, M.R. (2012). A 2in1 cloning system enables ratiometric bimolecular fluorescence complementation (rBiFC). Biotechniques **53:** 311–314.

Grefen, C., Karnik, R., Larson, E., Lefoulon, C., Wang, Y., Waghmare, S., Zhang, B., Hills, A., and Blatt, M.R. (2015). A vesicle-trafficking protein commandeers Kv channel voltage sensors for voltage-dependent secretion. Nat. Plants **1:** 15108–15119.

Hashimoto-Sugimoto, M., Higaki, T., Yaeno, T., Nagami, A., Irie, M., Fujimi, M., Miyamoto, M., Akita, K., Negi, J., Shirasu, K., Hasezawa, S., and Iba, K. (2013). A Munc13-like protein in Arabidopsis mediates H^+-ATPase translocation that is essential for stomatal responses. Nat. Commun. **4:** 2215.

Hecker, A., Wallmeroth, N., Peter, S., Blatt, M.R., Harter, K., and Grefen, C. (2015). Binary 2in1 vectors improve in planta (co-) localisation and dynamic protein interaction studies. Plant Physiol. **168:** 776–787.

Honsbein, A., Sokolovski, S., Grefen, C., Campanoni, P., Pratelli, R., Paneque, M., Chen, Z.H., Johansson, I., and Blatt, M.R. (2009). A tripartite SNARE-K+ channel complex mediates in channel-dependent K+ nutrition in Arabidopsis. Plant Cell **21:** 2859–2877.

Jahn, R., and Scheller, R.H. (2006). SNAREs--Engines for membrane fusion. Nat. Rev. Mol. Cell Biol. **7:** 631–643.

Kalmbach, L., Hématy, K., De Bellis, D., Barberon, M., Fujita, S., Ursache, R., Daraspe, J., and Geldner, N. (2017). Transient cell-specific EXO70A1 activity in the CASP domain and Casparian strip localization. Nat. Plants **3:** 17058.

Karnik, R., Grefen, C., Bayne, R., Honsbein, A., Köhler, T., Kioumourtzoglou, D., Williams, M., Bryant, N.J., and Blatt, M.R. (2013). Arabidopsis Sec1/Munc18 protein SEC11 is a competitive and dynamic modulator of SNARE binding and SYP121-dependent vesicle traffic. Plant Cell **25:** 1368–1382.

Karnik, R., Waghmare, S., Zhang, B., Larson, E., Lefoulon, C., Gonzalez, W., and Blatt, M.R. (2017). Commandeering channel voltage sensors for secretion, cell turgor, and volume control. Trends Plant Sci. **22:** 81–95.

Karnik, R., Zhang, B., Waghmare, S., Aderhold, C., Grefen, C., and Blatt, M.R. (2015). Binding of SEC11 indicates its role in SNARE recycling after vesicle fusion and identifies two pathways for vesicular traffic to the plasma membrane. Plant Cell **27:** 675–694.

Kulich, I., Pečenková, T., Sekereš, J., Smetana, O., Fendrych, M., Foissner, I., Höftberger, M., and Zárský, V. (2013). Arabidopsis exocyst subcomplex containing subunit EXO70B1 is involved in autophagy-related transport to the vacuole. Traffic **14:** 1155–1165.

Kulich, I., Vojtíková, Z., Sabol, P., Ortmannová, J., Neděla, V., Tihlaříková, E., and Žárský, V. (2018). Exocyst subunit EXO70H4 has a specific role in callose synthase secretion and silica accumulation. Plant Physiol. **176:** 2040–2051.

Kwon, C., et al. (2008). Co-option of a default secretory pathway for plant immune responses. Nature **451:** 835–840.

Lipka, V., Kwon, C., and Panstruga, R. (2007). SNARE-ware: The role of SNARE-domain proteins in plant biology. Annu. Rev. Cell Dev. Biol. **23:** 147–174.

Mei, K., and Guo, W. (2019). Exocytosis: A new exocyst movie. Curr. Biol. **29:** R30–R32.

Mei, K., et al. (2018). Cryo-EM structure of the exocyst complex. Nat. Struct. Mol. Biol. **25:** 139–146.

Morgera, F., Sallah, M.R., Dubuke, M.L., Gandhi, P., Brewer, D.N., Carr, C.M., and Munson, M. (2012). Regulation of exocytosis by the exocyst subunit Sec6 and the SM protein Sec1. Mol. Biol. Cell **23:** 337–346.

Pajonk, S., Kwon, C., Clemens, N., Panstruga, R., and Schulze-Lefert, P. (2008). Activity determinants and functional specialization of Arabidopsis PEN1 syntaxin in innate immunity. J. Biol. Chem. **283:** 26974–26984.

Pecenková, T., Hála, M., Kulich, I., Kocourková, D., Drdová, E., Fendrych, M., Toupalová, H., and Zársky, V. (2011). The role for the exocyst complex subunits Exo70B2 and Exo70H1 in the plant-pathogen interaction. J. Exp. Bot. **62:** 2107–2116.

Picco, A., Irastorza-Azcarate, I., Specht, T., Böke, D., Pazos, I., Rivier-Cordey, A.-S., Devos, D.P., Kaksonen, M., and Gallego, O. (2017). The in vivo architecture of the exocyst provides structural basis for exocytosis. Cell **168:** 400–412.

Pratelli, R., Sutter, J.U., and Blatt, M.R. (2004). A new catch in the SNARE. Trends Plant Sci. **9:** 187–195.

Ravikumar, R., Steiner, A., and Assaad, F.F. (2017). Multisubunit tethering complexes in higher plants. Curr. Opin. Plant Biol. **40:** 97–105.

Rehman, R.U., Stigliano, E., Lycett, G.W., Sticher, L., Sbano, F., Faraco, M., Dalessandro, G., and Di Sansebastiano, G.P. (2008). Tomato Rab11a characterization evidenced a difference between SYP121-dependent and SYP122-dependent exocytosis. Plant Cell Physiol. **49:** 751–766.

Reichardt, I., Slane, D., El Kasmi, F., Knöll, C., Fuchs, R., Mayer, U., Lipka, V., and Jürgens, G. (2011). Mechanisms of functional specificity among plasma-membrane syntaxins in Arabidopsis. Traffic **12:** 1269–1280.

Rossi, G., Lepore, D., Kenner, L., Czuchra, A.B., Plooster, M., Frost, A., Munson, M., and Brennwald, P. (2020). Exocyst structural changes associated with activation of tethering downstream of Rho/Cdc42 GTPases. J. Cell Biol. **219:** 219.

Sanderfoot, A.A., Assaad, F.F., and Raikhel, N.V. (2000). The Arabidopsis genome. An abundance of soluble N-ethylmaleimide-sensitive factor adaptor protein receptors. Plant Physiol. **124:** 1558–1569.

Schindelin, J., et al. (2012). Fiji: An open-source platform for biological-image analysis. Nat. Methods **9:** 676–682.

Shen, D., Yuan, H., Hutagalung, A., Verma, A., Kümmel, D., Wu, X., Reinisch, K., McNew, J.A., and Novick, P. (2013). The synaptobrevin homologue Snc2p recruits the exocyst to secretory vesicles by binding to Sec6p. J. Cell Biol. **202:** 509–526.

Sivaram, M.V.S., Saporita, J.A., Furgason, M.L.M., Boettcher, A.J., and Munson, M. (2005). Dimerization of the exocyst protein Sec6p and its interaction with the t-SNARE Sec9p. Biochemistry **44:** 6302–6311.

Südhof, T.C., and Rothman, J.E. (2009). Membrane fusion: Grappling with SNARE and SM proteins. Science **323:** 474–477.

Synek, L., Schlager, N., Eliás, M., Quentin, M., Hauser, M.-T., and Zárský, V. (2006). AtEXO70A1, a member of a family of putative exocyst subunits specifically expanded in land plants, is important for polar growth and plant development. Plant J. **48:** 54–72.

Synek, L., Sekereš, J., and Zárský, V. (2014). The exocyst at the interface between cytoskeleton and membranes in eukaryotic cells. Front Plant Sci **4:** 543.

Synek, L., Vukašinović, N., Kulich, I., Hála, M., Aldorfová, K., Fendrych, M., and Žárský, V. (2017). EXO70C2 is a key regulatory factor for optimal tip growth of pollen. Plant Physiol. **174:** 223–240.

TerBush, D.R., Maurice, T., Roth, D., and Novick, P. (1996). The exocyst is a multiprotein complex required for exocytosis in *Saccharomyces cerevisiae*. EMBO J. **15:** 6483–6494.

Tyrrell, M., Campanoni, P., Sutter, J.U., Pratelli, R., Paneque, M., Sokolovski, S., and Blatt, M.R. (2007). Selective targeting of plasma membrane and tonoplast traffic by inhibitory (dominant-negative) SNARE fragments. Plant J. **51:** 1099–1115.

Uemura, T., Sato, M.H., and Takeyasu, K. (2005). The longin domain regulates subcellular targeting of VAMP7 in *Arabidopsis thaliana*. FEBS Lett. **579:** 2842–2846.

Vukašinović, N., Oda, Y., Pejchar, P., Synek, L., Pečenková, T., Rawat, A., Sekereš, J., Potocký, M., and Žárský, V. (2017). Microtubule-dependent targeting of the exocyst complex is necessary for xylem development in Arabidopsis. New Phytol. **213:** 1052–1067.

Vukašinović, N., and Žárský, V. (2016). Tethering complexes in the Arabidopsis endomembrane system. Front. Cell Dev. Biol. **4:** 46.

Waghmare, S., Lefoulon, C., Zhang, B., Liliekyte, E., Donald, N., and Blatt, M.R. (2019). K^+ channel-SEC11 binding exchange regulates SNARE assembly for secretory traffic. Plant Physiol. **181:** 1096–1113.

Waghmare, S., Lileikyte, E., Karnik, R., Goodman, J.K., Blatt, M.R., and Jones, A.M.E. (2018). SNAREs SYP121 and SYP122 mediate the secretion of distinct cargo subsets. Plant Physiol. **178:** 1679–1688.

Walter, A., Silk, W.K., and Schurr, U. (2009). Environmental effects on spatial and temporal patterns of leaf and root growth. Annu. Rev. Plant Biol. **60:** 279–304.

Wang, W., Liu, N., Gao, C., Cai, H., Romeis, T., and Tang, D. (2020). The Arabidopsis exocyst subunits EXO70B1 and EXO70B2 regulate FLS2 homeostasis at the plasma membrane. New Phytol. **227:** 529–544.

Xia, L., Mar Marquès-Bueno, M., Bruce, C.G., and Karnik, R. (2019). Unusual roles of secretory SNARE SYP132 in plasma membrane H^+-ATPase traffic and vegetative plant growth. Plant Physiol. **180:** 837–858.

Xing, S., Wallmeroth, N., Berendzen, K.W., and Grefen, C. (2016). Techniques for the analysis of protein-protein interactions in vivo. Plant Physiol. **171:** 727–758.

Yue, P., Zhang, Y., Mei, K., Wang, S., Lesigang, J., Zhu, Y., Dong, G., and Guo, W. (2017). Sec3 promotes the initial binary t-SNARE complex assembly and membrane fusion. Nat. Commun. **8:** 14236.

Zárský, V., Cvrcková, F., Potocký, M., and Hála, M. (2009). Exocytosis and cell polarity in plants - Exocyst and recycling domains. New Phytol. **183:** 255–272.

Zárský, V., Kulich, I., Fendrych, M., and Pečenková, T. (2013). Exocyst complexes multiple functions in plant cells secretory pathways. Curr. Opin. Plant Biol. **16:** 726–733.

Zhang, B., Karnik, R., Alvim, J., Donald, N., and Blatt, M.R. (2019). Dual sites for SEC11 on the SNARE SYP121 implicate a binding exchange during secretory traffic. Plant Physiol. **180:** 228–239.

Zhang, B., Karnik, R., Donald, N., and Blatt, M.R. (2018). A GPI signal peptide-anchored split-ubiquitin (GPS) system for detecting soluble bait protein interactions at the membrane. Plant Physiol. **178:** 13–17.

Zhang, B., Karnik, R., Waghmare, S., Donald, N., and Blatt, M.R. (2017). VAMP721 conformations unmask an extended motif for K+ channel binding and gating control. Plant Physiol. **173:** 536–551.

Zhang, B., Karnik, R., Wang, Y., Wallmeroth, N., Blatt, M.R., and Grefen, C. (2015). The Arabidopsis R-SNARE VAMP721 interacts with KAT1 and KC1 K^+ Channels to Moderate K^+ current at the plasma membrane. Plant Cell **27:** 1697–1717.

Zhang, L., Zhang, H., Liu, P., Hao, H., Jin, J.B., and Lin, J. (2011). Arabidopsis R-SNARE proteins VAMP721 and VAMP722 are required for cell plate formation. PLoS One **6:** e26129.

Zhang, Z., Feechan, A., Pedersen, C., Newman, M.A., Qiu, J.L., Olesen, K.L., and Thordal-Christensen, H. (2007). A SNARE-protein has opposing functions in penetration resistance and defence signalling pathways. Plant J. **49:** 302–312.

Zhang, Z., Lenk, A., Andersson, M.X., Gjetting, T., Pedersen, C., Nielsen, M.E., Newman, M.A., Hou, B.H., Somerville, S.C., and Thordal-Christensen, H. (2008). A lesion-mimic syntaxin double mutant in Arabidopsis reveals novel complexity of pathogen defense signaling. Mol. Plant **1:** 510–527.